Chemical Engineering Journal 158 (2010) 271–280

Contents lists available at ScienceDirect

Chemical Engineering Journal

journal homepage: www.elsevier.com/locate/cej

Optimal trade-off design of integrated fermentation processes for ethanol production using genetically engineered yeast

Ming-Liang Chen, Feng-Sheng Wang*

Department of Chemical Engineering, National Chung Cheng University, 168 University Rd., Min-Hsiung, Chia-yi 621-02, Taiwan

ARTICLE INFO

Article history:
Received 8 August 2009
Received in revised form 20 January 2010
Accepted 21 January 2010

Keywords:
Recombinant yeast
Renewable fuel
Continuous fermentation
Fuzzy optimization
Sensitivity analysis
Hybrid differential evolution

ABSTRACT

In this study, we considered a multi-stage integrated extractive fermentation with cell recycling for ethanol production using the genetically engineered *Sacchromyces* yeast 1400 (pLNH33), which can utilize glucose and xylose as carbon sources to produce ethanol. Each stage consists of a stirred-tank bioreactor, a cell settler and an extractor. A generalized mathematical model was formulated to express the multi-stage integrated process. The aim of the optimization problem was to obtain the maximum overall productivity and conversions subject to the interval inequality constraints for the residual glucose and xylose concentrations and the total sugar supply. A fuzzy goal attainment method was applied to the multiobjective problem in order to achieve the maximum satisfaction for all design requirements. From the computational results, the integrated extractive fermentation with cell recycling (involving the extraction of ethanol from the extractor *in situ* to alleviate product inhibition) led to an optimal overall productivity that was 8.0% higher than that obtained by the method of continuous fermentation with cell recycling, and about 13-fold higher than that obtained by the method of continuous fermentation without cell recycling.

1. Introduction

Ethanol, one of the most important bio-fuels, can be produced by converting the sugar content of raw materials (e.g., corn, potatoes, beets, sugarcane, and wheat) to alcohol [1–4]. Today, there is heightened interest in ethanol as a transportation fuel. Ethanol production from renewable resources can improve energy security, reduce the accumulation of carbon dioxide, and decrease urban air pollution. When blended with gasoline, "neat" ethanol, as opposed to petroleum, would aid in stabilizing the concentration of smog-forming compounds in the atmosphere. Obtaining ethanol from lignocellulosic materials holds great promise as a new industry in the world and has the potential for making a significant contribution to the solution of major renewable energy and environmental problems [5–8].

Lignocellulosic feedstocks like wood, waste paper, agricultural residues and fast-growing energy crops have been identified as economical starting materials for ethanol production. These raw materials contain glucose and xylose as the major fermentable sugars. Although production of ethanol from the fermentation of hexose and pentose has been studied for many years, there are still several bottlenecks for the economical production of fuel ethanol. The fermentation of xylose to ethanol represents the main bottleneck in the production process. Several articles have reported the development of genetically engineered strains that utilize pentose and hexose as substrates in the production of ethanol [9–12].

Achieving a high ethanol production rate requires high cell concentrations in the bioreactor and maximization of the dilution rate. Continuous fermentation can increase productivity; however, it cannot be carried out in high cell density culture, which results in a low ethanol concentration and a significant loss of residual substrate [13]. To increase the efficiency of the ethanol fermentation process, various cell culture methods have been investigated [14–17]. A cell-recycling fermentation coupled with membrane filtering modules (for achieving a higher ethanol concentration) has gained considerable interest in recent years [18–21]. However, a high ethanol concentration may poison viable microorganisms and abrogate the fermentation process. Extractive fermentation is an alternative technique used to reduce end product inhibition by removing the fermentation product *in situ*. This technique is very simple and can be easily implemented with a large-scale fermentation system [22–26]. However, the toxicity of the organic solvent used in the removal of the end product is always a problem [27]. A biocompatible solvent should be employed to alleviate the poisoning of the microbe [28].

Lin and Wang [29] have introduced a multi-stage, integrated continuous fermentation process; each stage consists of a mixed tank, a bioreactor, a cell-recycling unit and an extractor used to pro-

* Corresponding author. Fax: +886 5 2721206.
E-mail address: chmfsw@ccu.edu.tw (F.-S. Wang).

1385-8947/$ – see front matter © 2010 Elsevier B.V. All rights reserved.
doi:10.1016/j.cej.2010.01.045

Nomenclature

b_l bleed ratio at the lth stage bioreactor
D_1 dilution rate at the first stage (h^{-1})
$D_{E,l}$ solvent dilution rate at the lth stage (h^{-1})
E_l extraction efficiency at the lth stage
F_l feed flow rate at the lth stage (m^3/h)
$F_{E,l}$ solvent flow rate at the lth stage (m^3/h)
f_k objective function and inequality constraint, $k = 1, \ldots, 6$
K extractive distribution coefficient
K_g, K_x saturation coefficient for cell growth on glucose and xylose, respectively (kg/m^3)
K'_g, K'_x saturation coefficient for ethanol production on glucose and xylose, respectively (kg/m^3)
K_{ig}, K_{ix} inhibition coefficient for cell growth on glucose and xylose, respectively (kg/m^3)
K'_{ig}, K'_{ix} inhibition coefficient for ethanol production on glucose and xylose, respectively (kg/m^3)
p_l ethanol concentration at the lth stage (kg/m^3)
p_{mg}, p_{mx} maximum ethanol concentration for cell growth on glucose and xylose, respectively (kg/m^3)
p'_{mg}, p'_{mx} maximum ethanol concentration for ethanol production on glucose and xylose, respectively (kg/m^3)
$s_{g,l}$, $s_{x,l}$ glucose and xylose concentration at the lth stage (kg/m^3)
s_{f_l} feed sugar concentration at the lth stage (kg/m^3)
$s^L_{g,r}$, $s^U_{g,r}$ lower and upper bounds of the residual glucose (kg/m^3)
$s^L_{x,r}$, $s^U_{x,r}$ lower and upper bounds of the residual xylose (kg/m^3)
s^L_t, s^U_t lower and upper bounds for the total sugar supply for the process (kg/m^3 h)
t time (h)
x_l, $s_{g,l}$, $s_{x,l}$, p_l cell, glucose, xylose and ethanol concentration inside the bioreactor at the lth stage (kg/m^3)
$x_{e,l}$, $s_{ge,l}$, $s_{xe,l}$, $p_{e,l}$ cell, glucose, xylose and ethanol concentration in the effluent at the lth stage (kg/m^3)
Y_{p/s_g}, Y_{p/s_x} yield coefficient for ethanol from glucose and xylose, respectively
z operation variables in the optimization problem

Greek symbols

α_l V_l/V_1, the volume ratio of the lth bioreactor to the first bioreactor
β_l F_l/F_1, the ratio of the overall feed flow rate at the lth stage to that at the first stage
$\chi_{g,l}$, $\chi_{x,l}$ glucose and xylose conversions at the lth stage
$\delta_{x,l}$, $\delta_{s,l}$, $\delta_{p,l}$ separation factor for cell, substrate and ethanol at the lth stage
ε_l recycle ratio for the lth cell settler
ϕ_g, ϕ_x power of ethanol inhibition for cell growth on glucose and xylose, respectively
φ_g, φ_x power of ethanol inhibition for ethanol production on glucose and xylose, respectively
η_D aggregation function
$\eta_k(f_k)$ membership function for each of the objective functions
λ linear combination ratio for the fed glucose concentration to the fed sugar concentration
μ_g, μ_x specific cell growth rate for yeast 1400 (pLNH33) on glucose and xylose, respectively
μ_{mg}, μ_{mx} maximum specific growth rate coefficient for yeast 1400 (pLNH33) on glucose and xylose, respectively (h^{-1})
ν_g, ν_x specific ethanol production rate for yeast 1400 (pLNH33) on glucose and xylose, respectively
ν_{mg}, ν_{mx} coefficient of maximum specific ethanol production rate for yeast 1400 (pLNH33) on glucose and xylose, respectively (h^{-1})
π_l ethanol productivity at the lth stage (kg/m^3 h)
$\zeta_{x,l}$ discarded factor for cell at the lth stage
$\zeta_{sg,l}$, $\zeta_{sx,l}$, $\zeta_{p,l}$ condensed factor for glucose, xylose and ethanol at the lth stage

Subscript

* optimal solution

duce lactic acid. A membrane filter was employed in the integrated process so that the filtrate was assumed to be cell-free. In this study, we will introduce a modification to the integrated process that uses the genetically engineered *Saccharomyces* yeast 1400 (pLNH33) to produce ethanol. The yeast 1400 (pLNH33) has a self-flocculating characteristic that enables us to use a cheaper settler as a cell separator to replace the expensive membrane separation unit; the yeast can also utilize xylose and glucose to produce ethanol. In this study, we reformulate the mathematical model to describe characteristics of the integrated extractive fermentation process using hexose and pentose to maximize ethanol productivity. Several design parameters, such as the dilution rate, the fed sugar concentrations and the bleed ratio, should be considered in the integrated process. Sensitivity analysis is applied to determine which operation variables are the most relevant in the process. The fuzzy goal attainment method will be introduced to design the integrated extraction fermentation processes.

2. Process formulation

A schematic drawing of the multi-stage, integrated extractive fermentation process is shown in Fig. 1. Each stage consists of a stirred-tank bioreactor, a cell settler and an extractor. The sterile glucose, xylose and nutrient media are well stirred in the mixing tank to form a homogeneous substrate, which is continuously fed into each bioreactor. The genetically engineered *Sacchromyces* yeast 1400 (pLNH33) [30] can utilize the glucose and xylose to produce ethanol. Small amounts of the outlet of each bioreactor are fed into the next bioreactor, but the rest flows into a cell settler while maintaining a constant temperature of 42 °C throughout. The yeast 1400 (pLNH33) quickly flocculates at that temperature. The density of self-flocculated yeast is greater than that of the broth, so the yeast settle down to the bottom. The original characteristics of the yeast 1400 (pLNH33) are restored and they are recycled back to the bioreactor when a constant temperature of 30 °C is maintained. As a result, the bioreactor can retain a high cell density culture. The clear fluid is overflowed into an extractor to take off the ethanol. A biocompatible solvent, such as an isopropyl pentyl ketone, is added to the extractor to extract ethanol [31]. The solvent should be biocompatible, inert to the reaction, stable under the liquid-phase reaction conditions, easy to separate from ethanol and able to induce phase splitting. The raffinate phase in the extractor, containing some unconverted substrate, ethanol and solvent, is also transferred to the next bioreactor.

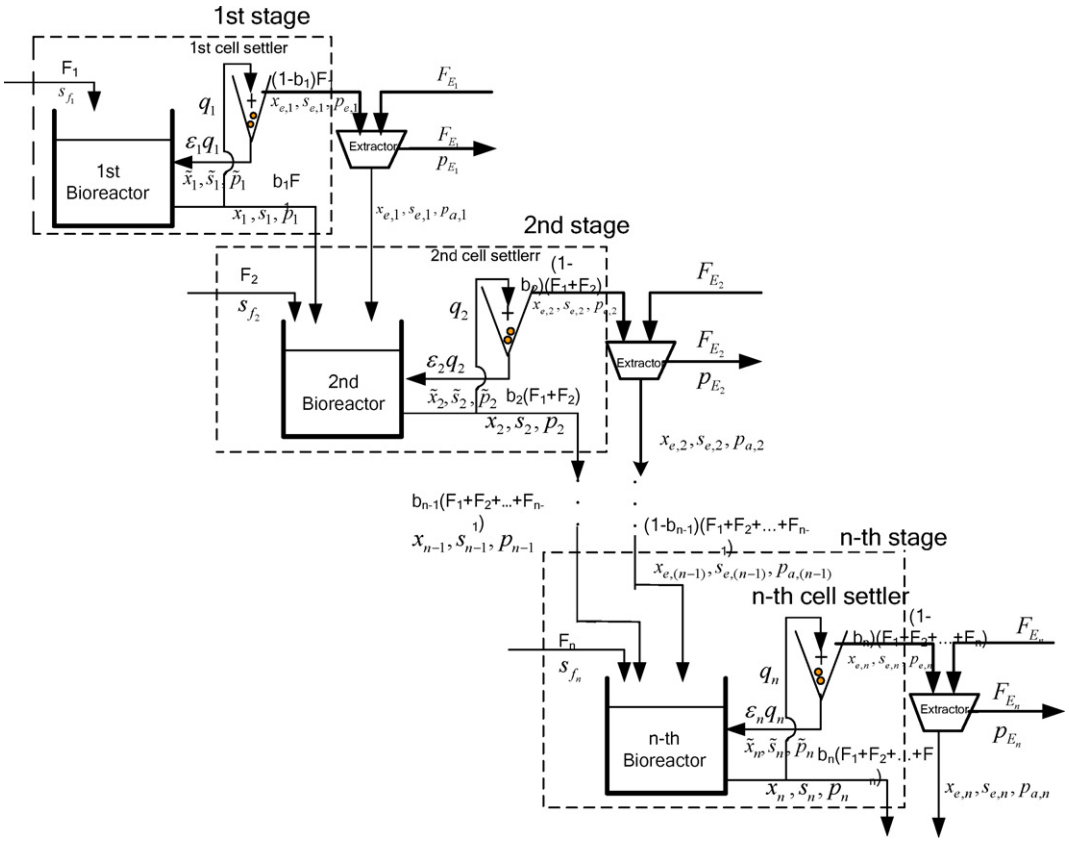

Fig. 1. Schematic diagram of a multi-stage integrated extractive fermentation process. Each stage consists of a bioreactor, a settler unit for cell recycling and an extractor.

2.1. Material balance equations

The material balance equations for the recombinant yeast 1400 (pLNH33) in glucose and xylose mixtures around the first stage, as shown in a dashed box of Fig. 1, are expressed as follows:

$$\frac{dx_1}{dt} = -D_1\left[b_1 + (1-b_1)\frac{1-\varepsilon_1\delta_{x,1}}{1-\varepsilon_1}\right]x_1 + r_{x,1} \tag{1}$$

where $D_1 = F_1/V_1$ is the dilution rate, b_1 is the bleed ratio at the first stage and ε_1 is the recycle ratio for the first cell settler. Both the bleed ratio and recycle ratio are restricted between zero and one. The cell growth rate, $r_{x,1}$, for the recombinant yeast 1400 (pLNH33) at the first stage will be discussed in the following section. The second terms in the bracket of Eq. (1) are obtained from the material balance equation around the cell settler. Note that the balance equation is different from that discussed in Lin and Wang [29]. We suppose that the recycled cell concentration is condensed as the ratio $\delta_{x,1} = \tilde{x}_1/x_1$. The cell separation factor, $\delta_{x,1}$, at the first cell settler must be restricted to within $1 \le \delta_{x,1} \le 1/\varepsilon_1$. The yeast 1400 (pLNH33) can quickly flocculate and settle down in the cell settler at the temperature over 42 °C. Using material balance equations at the cell settler, we obtain the cell discarded factor as

$$\zeta_{x,1} = \frac{x_{e,1}}{x_1} = \frac{1-\varepsilon_1\delta_{x,1}}{1-\varepsilon_1} \tag{2}$$

The cell separation factor or cell discarded factor is expressed in terms of the characteristics of the flocculated cell. Eq. (2) indicates the relationship between both factors such that we need to assign only one of the factors for the design of the process.

Following procedures similar to those discussed above, the material balance equations for glucose, $s_{g,1}$, and xylose, $s_{x,1}$, respectively, are expressed as

$$\frac{ds_{g,1}}{dt} = D_1\left\{s_{gf,1} - \left[b_1 + (1-b_1)\frac{1-\varepsilon_1\delta_{s,1}}{1-\varepsilon_1}\right]s_{g,1}\right\} - r_{s_{g,1}} \tag{3}$$

$$\frac{ds_{x,1}}{dt} = D_1\left\{s_{xf,1} - \left[b_1 + (1-b_1)\frac{1-\varepsilon_1\delta_{s,1}}{1-\varepsilon_1}\right]s_{x,1}\right\} - r_{s_{x,1}} \tag{4}$$

The gluose and xylose are well stirred in the mixing tank to form a homogeneous substrate so that the fed glucose concentration $s_{g_{f,1}}$ and fed xylose concentration $s_{x_{f,1}}$ can be respectively expressed as $s_{g_{f,1}} = \lambda s_{f_1}$ and $s_{x_{f,1}} = (1-\lambda)s_{f_1}$, where λ is the linear combination ratio. The monosaccharide separation factor is restricted by $0 \le \delta_{s,1} \le 1$, which is different from that of the cell separation factor. The glucose and xylose consumption rates, $r_{s_{g,1}}$ and $r_{s_{x,1}}$, at the first stage will be discussed in the following section. Ethanol is produced from glucose and xylose mixtures so that the formation rate is expressed as the sum of the ethanol formation rates from glucose and xylose, i.e., $dp/dt = dp_g/dt + dp_x/dt$, where p_g and p_x are the ethanol concentrations formed from glucose and xylose, respectively. The material balance equations for ethanol formed are expressed as

$$\frac{dp_1}{dt} = -D_1\left[b_1 + (1-b_1)\frac{1-\varepsilon_1\delta_{p,1}}{1-\varepsilon_1}\right]p_1 + r_{p_1} \tag{5}$$

where the ethanol separation factors are restricted by $0 \le \delta_{p,1} \le 1$. Similarly, using material balance equations at the cell settler, we obtain the substrate and ethanol condensed factors of

$$\zeta_{s,1} = \frac{s_{e,1}}{s_1} = \frac{1-\varepsilon_1\delta_{s,1}}{1-\varepsilon_1} \tag{6}$$

$$\zeta_{p,1} = \frac{p_{e,1}}{p_1} = \frac{1-\varepsilon_1\delta_{p,1}}{1-\varepsilon_1} \tag{7}$$

Similarly, the material balance equations for the recombinant yeast, glucose, xylose and ethanol around the lth stage are described as follows:

$$\frac{dx_l}{dt} = \frac{D_1}{\alpha_l}\left[\left(\sum_{i=1}^{l-1}\beta_i\right)\left(b_{l-1}+(1-b_{l-1})\zeta_{x,l-1}\right)x_{l-1} - \left(\sum_{i=1}^{l}\beta_i\right)\left(b_l+(1-b_l)\zeta_{x,l}\right)x_l\right] + r_{x,l} \quad (8)$$

$$\frac{ds_{g,l}}{dt} = \frac{D_1}{\alpha_l}\left[\beta_l s_{g_{f,1}} + \left(\sum_{i=1}^{l-1}\beta_i\right)\left(b_{l-1}+(1-b_{l-1})\zeta_{s_g,l-1}\right)s_{g,l-1} - \left(\sum_{i=1}^{l}\beta_i\right)\left(b_l+(1-b_l)\zeta_{s_g,l}\right)s_{g,l}\right] - r_{s_{g,l}} \quad (9)$$

$$\frac{ds_{x,l}}{dt} = \frac{D_1}{\alpha_l}\left[\beta_l s_{x_{f,1}} + \left(\sum_{i=1}^{l-1}\beta_i\right)(b_{l-1}+(1-b_{l-1})\zeta_{s_x,l-1})s_{x,l-1} - \left(\sum_{i=1}^{l}\beta_i\right)\left(b_l+(1-b_l)\zeta_{s_x,l}\right)s_{x,l}\right] - r_{s_{x,l}} \quad (10)$$

$$\frac{dp_l}{dt} = \frac{D_1}{\alpha_l}\left[\left(\sum_{i=1}^{l-1}\beta_i\right)\left(b_{l-1}+(1-b_{l-1})\frac{\zeta_{p,l-1}}{(1+E_{l-1})}\right)p_{l-1} - \left(\sum_{i=1}^{l}\beta_i\right)\left(b_l+(1-b_l)\zeta_{p,l}\right)p_l\right] + r_{p_l}; \quad l=1,\ldots,n \quad (11)$$

where $\beta_l = F_l/F_1$ is the ratio of the flow rate at the lth stage to the flow rate at the first stage, $\alpha_l = V_l/V_1$ is the volume ratio of the lth bioreactor to the first bioreactor, b_l is the bleed ratio at the lth stage, $\zeta_{x,l}$, $\zeta_{sg,l}$, $\zeta_{sx,l}$ and $\zeta_{p,l}$ are the cell discarded factor and glucose, xylose and ethanol condensed factors at the lth stage.

The supernatant at the previous cell settler is overflowed to an extractor to remove ethanol. The material balance for ethanol at the lth extractor can be written as

$$(1-b_l)D_1 p_{e,l}\sum_{i=1}^{l}\beta_i - D_{E,l}p_{E,l} - (1-b_l)D_1\frac{p_{e,l}}{1+E_l}\sum_{i=1}^{l}\beta_i = 0 \quad (12)$$

where the solvent dilution rate is defined as $D_{E,l} = F_{E,l}/V_1$, and $F_{E,l}$ is the solvent flow rate at the lth stage. The extraction efficiency, E_l, at the lth stage is defined as

$$E_l = \frac{p_{e,l}}{p_{a,l}} - 1 = \frac{KD_{E,l}}{(1-b_l)D_l} \quad (13)$$

where K is the extractive distribution coefficient. The process formulation is simplified to the integrated fermentation process discussed by Lin and Wang [29] if the cell discarded factor for each stage is zero and both substrate and ethanol condensed factors are set to one.

2.2. Kinetic models

The reaction rates in the material balance equations, (1), (3)–(5) and (8)–(11), are in terms of the employed microbial species and are calculated at each stage. In this work, we consider the genetically engineered *Sacchromyces* yeast 1400 (pLNH33) as the microbial species that produces ethanol. The recombinant *Saccharomyces* yeast 1400 (pLNH33) was developed by cloning the xylose reductase and xylitol dehydrogenase genes from *Pichia stipitis* and over-expressing the xylulokinase activity of the host yeast (the fusion product yeast 1400) [32]. The recombinant yeast 1400 (pLNH33) utilizes glucose and xylose simultaneously. The recombinant plasmids in 1400 (pLNH33) may be lost by natural processes during fermentation. However, the parent yeast 1400 utilizes glucose only. Krishnan et al. [33] has developed a kinetic model to describe the cell growth and product formation of the yeast 1400 (pLNH33) on glucose and xylose mixtures. The specific cell growth rates for the yeast 1400 (pLNH33) on glucose and xylose, respectively, are expressed by

$$\mu_g = \frac{\mu_{mg}s_g}{K_g + s_g + (s_g^2/K_{i,g})}\left\{1-\left(\frac{p_g}{p_{mg}}\right)^{\phi_g}\right\} \quad (14)$$

$$\mu_x = \frac{\mu_{mx}s_x}{K_x + s_x + (s_x^2/K_{i,x})}\left\{1-\left(\frac{p_x}{p_{mx}}\right)^{\phi_x}\right\} \quad (15)$$

The specific cell growth rate for the yeast 1400 (pLNH33) on glucose and xylose mixtures is approximated by

$$\mu_{mix} = \frac{s_g}{s_g+s_x}\mu_g + \frac{s_x}{s_g+s_x}\mu_x \quad (16)$$

The specific production rates for the yeast 1400 (pLNH33) on glucose and xylose, respectively, are in the forms

$$\nu_g = \frac{\nu_{mg}s_g}{K'_g + s_g + (s_g^2/K'_{i,g})}\left\{1-\left(\frac{p_g}{p'_{mg}}\right)^{\varphi_g}\right\} \quad (17)$$

$$\nu_x = \frac{\nu_{mx}s_x}{K'_x + s_x + (s_x^2/K'_{i,x})}\left\{1-\left(\frac{p_x}{p'_{mx}}\right)^{\varphi_x}\right\} \quad (18)$$

The reaction rates described in material balance equations are therefore expressed as follows:

$$r_x = \mu_{mix}x \quad (19)$$

$$r_p = \left(\nu_g + \nu_x\right)x \quad (20)$$

$$r_{s_g} = \frac{1}{Y_{p/s_g}}\nu_g x \quad (21)$$

$$r_{s_x} = \frac{1}{Y_{p/s_x}}\nu_x x \quad (22)$$

Here the notations in (14)–(22) are expressed in the nomenclature section of this paper, and their kinetic parameter values are taken from Krishnan et al. [33].

3. Optimization

3.1. Objectives and constraints

The aim of the optimization problem is to maximize the overall ethanol productivity and the overall glucose and xylose conversions simultaneously. The problem is therefore formulated as a multiobjective optimization problem (MOOP) in the forms

Overall ethanol productivity:

$$\max_z f_1 = \frac{D_1}{\sum_{i=1}^{n}\alpha_i}\left[\left(\sum_{j=1}^{n}\beta_j\right)\left(b_n+(1-b_n)\zeta_{p,n}\right)p_n + \sum_{i=1}^{n-1}(1-b_i)\frac{\zeta_{p,i}E_i}{(1+E_i)}\left(\sum_{j=1}^{i}\beta_j\right)p_i\right] \quad (23)$$

Overall glucose conversion:

$$\max_z f_2 = 1 - \frac{\left(\sum_{i=1}^{n}\beta_i\right)\left(b_n + (1-b_n)\zeta_{s_g,n}\right)s_{g,n}}{\left(\sum_{i=1}^{n}\beta_i s_{g_{f,i}}\right)} \tag{24}$$

Overall xylose conversion:

$$\max_z f_3 = 1 - \frac{\left(\sum_{i=1}^{n}\beta_i\right)\left(b_n + (1-b_n)\zeta_{s_x,n}\right)s_{x,n}}{\left(\sum_{i=1}^{n}\beta_i s_{x_{f,i}}\right)} \tag{25}$$

where the operation variable, $\mathbf{z}$, consists of the dilution rate, D_1, the fed sugar concentrations, s_{f_l} (which is the linear combination of fed glucose and xylose concentrations), and the bleed ratio, b_l, at each stage. The operation variables are restricted to within physically realistic boundaries, as in the forms

$$\mathbf{z}_{\min} \le \mathbf{z} = \left[D_1, s_{f_1}, \ldots, s_{f_n}, b_1, \ldots, b_n\right] \le \mathbf{z}_{\max} \tag{26}$$

Nearly all engineering processes require the consideration of some physical constraints. The productivity and conversion at each stage must be non-negative.

Productivity at lth stage:

$$\pi_l = \frac{D_1}{\alpha_l}\left[\left(\sum_{i=1}^{l}\beta_i\right)\left(b_l + (1-b_l)\zeta_{p,l}\right)p_l - \left(\sum_{i=1}^{l-1}\beta_i\right) \times \left(b_{l-1} + \frac{1-b_{l-1}}{1+E_{l-1}}\zeta_{p,l-1}\right)p_{l-1}\right] \ge 0 \quad l = 1, \ldots, n \tag{27}$$

Glucose conversion at lth stage:

$$\chi_{g,l} = 1 - \frac{\left(\sum_{i=1}^{l}\beta_i\right)\left(b_l + (1-b_l)\zeta_{s_g,l}\right)s_{g,l}}{\beta_l \lambda s_{f_l} + \left(\sum_{i=1}^{l-1}\beta_i\right)\left(b_{l-1} + (1-b_{l-1})\zeta_{s_g,l}\right)s_{g,l-1}} \ge 0 \quad l = 1, \ldots, n \tag{28}$$

Xylose conversion at lth stage:

$$\chi_{x,l} = 1 - \frac{\left(\sum_{i=1}^{l}\beta_i\right)\left(b_l + (1-b_l)\zeta_{s_x,l}\right)s_{x,l}}{\beta_l (1-\lambda) s_{f_l} + \left(\sum_{i=1}^{l-1}\beta_i\right)\left(b_{l-1} + (1-b_{l-1})\zeta_{s_x,l}\right)s_{x,l-1}} \ge 0 \quad l = 1, \ldots, n \tag{29}$$

where λ is the fraction of the fed glucose concentration.

High productivity and conversion are the main goals of fermentation industrials to produce commodity chemicals. However, the total amount of the raw materials, such as glucose and xylose, supplied for the fermentation process needs to be restricted in order to limit the investment cost. The total sugar supply is therefore restricted by

$$\frac{D_1\left(\sum_{i=1}^{n}\beta_i s_{f_i}\right)}{\left(\sum_{i=1}^{n}\alpha_i\right)} \le s_t^B \tag{30}$$

where s_t^B is the crisp boundary for the supplied sugar flux. This boundary is equivalent to the total amount of glucose and xylose supplied to the process, which is one of the investment costs. To reduce the separation cost and environmental impact, two additional inequality constraints are considered to restrict the residual glucose and xylose in the final stage as

$$s_{g,n} \le s_{g,r}^B \tag{31}$$

$$s_{x,n} \le s_{x,r}^B \tag{32}$$

where $s_{g,r}^B$ and $s_{x,r}^B$ are the crisp boundaries for the desired residual glucose and xylose, which are used to limit the operation cost in a follow-up ethanol separation process. The boundary values, s_t^B, $s_{g,r}^B$ and $s_{x,r}^B$, must be assigned by a designer prior to solving the MOOP.

Much of the MOOP in the real world takes place in an environment in which the designer knows the preferred goals and boundaries in advance. Such a preference design problem is a branch of decision-making problems. The weighted sum method is a commonly used technique for solving a MOOP to obtain a Pareto-optimal solution [34–36]. However, the weighted sum method is not a preference technique, so the method cannot accommodate the designer's pre-assigned preferred goals and boundaries. Some preference techniques, such as nonlinear goal programming, compromise programming and surrogate worth trade-off methods, can be employed to solve the decision-making problem [35,36]. Such methods can be applied to solve crisp preference goals and boundaries. However, in real-world applications, the goal for each objective function and the boundary for each constraint are, in general, interval boundaries rather than rigid values, so the problem becomes a fuzzy or flexible optimization problem. Here, we introduced a fuzzy goal attainment method to solve the optimal design problem with an interval preference goal and boundaries towards obtaining a compromise design.

3.2. Fuzzy goal attainment problem

The goal for each objective function and the boundary for each constraint are, in general, interval boundaries, not rigid values. Such an optimization problem can be formulated as a fuzzy optimization problem [28,29,37,38]; that is, the designer can assign the interval preferred goals, $\left[f_k^L, f_k^U\right]$, $k = 1, 2, 3$, for each objective function in Eqs. (23)–(25) and the interval boundaries, $\left[f_k^L, f_k^U\right]$, $k = 4, 5, 6$, for each constraint in Eqs. (30)–(32). In contrast to the above crisp optimization problem, we soften the rigid requirements to strictly maximize the objective functions and to strictly satisfy the constraints. As a result, the optimization problem is softened into the following fuzzy preference goal problem

$$\text{fuzzy } \max_{z\in\Omega} f_1 \gtrsim \left[f_1^L, f_1^U\right] \tag{33}$$

$$\text{fuzzy } \max_{z\in\Omega} f_2 \gtrsim \left[f_2^L, f_2^U\right] \tag{34}$$

$$\text{fuzzy } \max_{z\in\Omega} f_3 \gtrsim \left[f_3^L, f_3^U\right] \tag{35}$$

Here, the symbol "$\gtrsim$" denotes a relaxed or fuzzy version of the ordinary inequality "$\ge$". The crisp set of constraints, Ω, consists of the material balance equations of the process. The fuzzy maximization means that the design is completely acceptable if the productivity and conversions are greater than each corresponding upper bound, f_k^U. Conversely, the design is completely unacceptable if the maximum productivity and conversions are less than the lower bound f_k^L. When the productivity and conversions are between the intervals $\left[f_k^L, f_k^U\right]$, $k = 1, 2, 3$, this implies that the design criteria are acceptable for some satisfaction.

The fuzzy inequality constraints are expressed as:

$$f_4 = \frac{D_1\left(\sum_{i=1}^{n}\beta_i s_{f_i}\right)}{\left(\sum_{i=1}^{n}\alpha_i\right)} \precsim \left[s_t^L, s_t^U\right] = \left[f_4^L, f_4^U\right] \tag{36}$$

$$f_5 = s_{g,n} \precsim \left[s_{g,r}^L, s_{g,r}^U\right] = \left[f_5^L, f_5^U\right] \tag{37}$$

$$f_6 = s_{x,n} \precsim \left[s_{x,r}^L, s_{x,r}^U\right] = \left[f_6^L, f_6^U\right] \tag{38}$$

where the symbol "$\precsim$" denotes a relaxed or fuzzy version of the ordinary inequality "$\le$", and $[f_k^L, f_k^U]$, $k = 4, 5, 6$ are the interval boundaries. The fuzzy inequality constraint means that the design is completely acceptable if both sugar supply and the residual glucose and xylose concentrations are less than the lower bounds,

f_k^L, $k = 4, 5, 6$. Conversely, the design is completely unacceptable if both sugar supply and residual glucose and xylose concentrations are greater than the upper bound, f_k^U, $k = 4, 5, 6$. When the sugar supply and residual glucose and xylose concentrations are between the intervals $\left[f_k^L, f_k^U\right]$, $k = 4, 5, 6$, the design is acceptable for some satisfaction.

The fuzzy goals for the ethanol productivity and conversion can be quantified by eliciting membership functions from the designer. The fuzzy maximization is stated such that the designer aims to both achieve target values "substantially greater than or equal to some interval" and determine the subjective membership function, which is a strictly monotonically increasing function with respect to f_k in the following way:

$$\eta_k(f_k) = \begin{cases} 0; & f_k \le f_k^L, \quad k = 1, 2, 3 \\ d_k; & f_k^L \le f_k \le f_k^U \\ 1; & f_k^U \le f_k \end{cases} \tag{39}$$

where f_k^L or f_k^U represents the value of f_k such that the grade of the membership function $\eta_k(f_k)$ is 0 or 1 and the grades of the membership for the intermediate function values are expressed by a strictly monotonically increasing function, d_k, with respect to f_k.

For treating fuzzy inequality constraints, we proposed the following membership functions:

$$\eta_k(f_k) = \begin{cases} 1, & f_k \le f_k^L, \quad k = 4, 5, 6 \\ d'_k, & f_k^L \le f_k \le f_k^U \\ 0, & f_k \ge f_k^U \end{cases} \tag{40}$$

where f_k^L or f_k^U represents the value of f_k such that the grade of the membership function, $\eta_k(f_k)$, is 1 or 0 and the grades of the membership for the intermediate function values are expressed by a strictly monotonically decreasing function, d'_k, with respect to f_k. If both objective functions and inequality constraints are less than their lower bounds, the intersection for both membership functions is zero. Conversely, if both objective functions and inequality constraints are greater than the upper bounds, the intersection for both membership functions is still zero. The aim of fuzzy optimization is therefore to find a maximum intersection for all membership functions and desired boundaries within the preference intervals.

Having elicited the membership functions from the designer for each objective function and constraint, the fuzzy optimization problem can be expressed as a maximizing fuzzy goal attainment problem in the form

$$\min_{z \in \Omega} \eta_D = \min_{z \in \Omega} \left[\max_{k=1,2,3,4,5,6} \left\{ \bar{\eta}_k - \eta_k(f_k) \right\} + \rho \sum_{k=1}^{6} (\bar{\eta}_k - \eta_k(f_k)) \right] \tag{41}$$

where η_D denotes an aggregation function defined on the crisp search domain, Ω. Several aggregation functions were introduced in the textbook by Sakawa [36]. The value of the aggregation function can be interpreted as a representation of the overall satisfaction with the designer's fuzzy goals. The first term of the aggregation function is applied to determine the optimal trade-off solution that is nearest to the ideal preference goal, $\bar{\eta}_k$, which indicates 100% satisfaction. The second term is employed to avoid inspection of a unique test for optimality, in which the constant ρ is a sufficiently small positive value in the range of 10^{-3}–10^{-5}. The fuzzy goal attainment approach is applied to find a satisfactory solution to the Pareto set without yielding the Pareto frontier of the problem.

4. Results and discussion

Hybrid differential evolution (HDE) is applied to solve the fuzzy goal attainment problem (41) to obtain a Pareto-optimal solution. All the computations were performed on a personal computer, Intel Core 2 CPU 2.13 GHz, using Microsoft Windows XP. The HDE algorithm was implemented on Compaq Visual Fortran, and has to be provided with four setting factors as follows: the crossover factor was set to 0.5, two tolerances used in the migration were set to 0.05, and a population size of 5 was used for all runs. In HDE, the mutation factor is taken as a random number within [0, 1]. We applied HDE with a multiplier-updating method that included an adaptive penalty parameter strategy to solve the constrained problem. The initial penalty parameters were set to 10^3. HDE has been successfully applied in several chemical process optimization problems [28,29,31,37–39]. The HDE algorithm was discussed in detail by Chiou and Wang [39]. To solve the fuzzy goal attainment problem, we used the exponential membership function to judge the fuzzy preference for each of the objective functions and inequality constraints. For each run, it was necessary to assign preference interval boundaries for each objective function and inequality constraint, as listed in Table 1. In the example, the reference membership levels, $\bar{\eta}_k$, were set to one for each objective function and inequality constraint. This means that the designer would like to achieve 100% satisfaction for each objective function and inequality constraint. A determinant in finding a feasible solution to the fuzzy goal attainment problem is the assignment of realizable preference interval boundaries. Such preference interval boundaries are chosen in terms of the designer's experience with the process. It is not possible to find a solution satisfying all objective functions and constraints if the assigned values are too strict. As a result, at least one of the membership functions should be zero so the optimal decision η_D^* is equal to one. If the optimal decision η_D^* is between zero and one, this implies that each membership function value $\eta_k(f_k)$ is also between zero and one. This situation indicates that the design satisfies the optimal solution to some degree.

Table 1
The optimal results for the three-stage integrated extractive fermentation process with various operation variables. The preference interval boundaries for objective function are assigned as $\left[f_1^L, f_1^U\right] = [5.0, 20.0]$ and $\left[f_2^L, f_2^U\right] = \left[f_3^L, f_3^U\right] = [0.95, 1.0]$, and interval boundaries for constraints as $\left[f_4^L, f_4^U\right] = [10, 40]$, $\left[f_5^L, f_5^U\right] = [0.1, 0.5]$ and $\left[f_6^L, f_6^U\right] = [0.5, 1.0]$. The values in parentheses indicate the optimal grades of the membership function for each objective and constraint.

Case	1	2	3	4
Productivity (kg/m^3 h)	4.249 (0.0)	6.311 (0.132)	11.748 (0.573)	11.761 (0.574)
Glucose conversion	1.0 (1.0)	1.0 (1.0)	1.0 (1.0)	1.0 (1.0)
Xylose conversion	0.903 (0.0)	0.970 (0.527)	0.984 (0.784)	0.991 (0.882)
Sugar supply (kg/m^3 h)	9.836 (1.0)	14.299 (0.910)	26.503 (0.573)	26.477 (0.574)
Residual glucose conc. (kg/m^3)	3.906E−4 (1.0)	5.889E−5 (1.0)	4.539E−5 (1.0)	1.827E−5 (1.0)
Residual xylose conc. (kg/m^3)	1.340 (0.0)	0.956 (0.132)	0.370 (1.0)	0.169 (1.0)
Dilution rate (h^{-1})	0.738	0.463	1.177	1.716
Fed sugar conc. (kg/m^3)	40.0	92.603	67.532	52.790
Bleed ratio for each stage	0.2, 0.2, 0.2	0.2, 0.2, 0.2	0.077, 0.077, 0.077	0.041, 0.051, 0.057
Volume ratio	1.0, 1.0, 1.0	1.0, 1.0, 1.0	1.0, 1.0, 1.0	1.0, 1.24, 1.18

Operation parameters are set as $\alpha_1 = \alpha_2 = \alpha_3 = 1$, $\beta_1 = 1$, $\beta_2 = \beta_3 = 0$, $E_1 = E_2 = E_3 = 6.93$, $\zeta_x = 0.01$, $\zeta_s = \zeta_p = 1.01$, $\varepsilon_1 = \varepsilon_2 = \varepsilon_3 = 0.95$, and $\lambda = 0.65$.

Table 1 shows the optimal solutions of a three-stage integrated process using the various operation variables. In the first case, we considered the dilution rate as the operation variable and set the other operation variables as $s_{f_1} = 40\,\text{kg/m}^3$ and $b_1 = b_2 = b_3 = 0.2$, i.e., the sugar is fed into the first bioreactor only, and the bleed ratios are identical for each stage. The optimal dilution rate of $0.738\,\text{h}^{-1}$ was obtained by HDE. We obtained a total sugar supply of $9.836\,\text{kg/m}^3$ h and retained the residual glucose concentration of 3.906E−4 kg/m^3 and xylose concentration of $1.340\,\text{kg/m}^3$, which is greater than the assigned upper bound, to yield the maximum overall ethanol productivity of $4.249\,\text{kg/m}^3$ h, overall glucose conversion of 1.0 and overall xylose conversion of 0.903. The overall ethanol productivity and xylose conversion are less than their desired lower bounds and residual xylose concentration is more than the desired upper bound. As a result, the membership grades for the objectives and constraint were zero. This result implies that the design was completely unacceptable, because these objective functions and constraints have a 0% satisfactory solution.

In the second case, the dilution rate and fed sugar concentration are considered to be the operation variables, i.e., $z = \left[D_1, s_{f_1}\right]$, and the other operation conditions are the same as those of the first case. The optimal dilution rate decreased about 63% and the fed glucose concentration increased about 2.32-fold relative to that of the first case so that the maximum productivity obtained ($6.311\,\text{kg/m}^3$ h) increased by 148% over that of Case 1. In this case, the objective function values and constraints are within their desired interval boundaries, so that we obtain a 13.2% satisfactory solution for all objective functions and constraints. In the third case, we considered the bleed ratio for each stage to be equal (i.e., as a single design variable), so that the operation variables considered in this case were $\boldsymbol{z} = \left[D_1, s_{f_1}, b_1\right]$. The optimal dilution rate of $1.214\,\text{h}^{-1}$ was obtained by HDE. We obtained the total sugar supply of $26.503\,\text{kg/m}^3$ h and retained the residual glucose concentration of 4.473E−5 kg/m^3 and xylose concentration of $0.357\,\text{kg/m}^3$ to yield the maximum overall ethanol productivity of $11.749\,\text{kg/m}^3$ h. In this case, we obtain a 57.3% satisfactory solution for all objective functions and constraints. HDE with 10,000 generations was applied to solve each case. The optimal solution for Case 3 is reached using the total objective function call of 50,166 which is equivalent to the CPU time of about 10.8 h on a personal computer. The main computational time spends for solving differential equations (about 10.3 h) towards achieving the steady-state values for evaluating the objective functions and constraints. In this study, the subroutine IVMRK in IMSL Math/Library, which uses Runge–Kutta pairs of various orders, is applied to solve differential equations.

This multiobjective optimization problem (MOOP) involves a set of operation variables as expressed in Eq. (26). In many cases, the decision-maker would be interested in knowing the sensitivities of the optimal design with respect to the operation variables. This situation indicates that the decision-maker would like to know variations to the optimal overall productivity, conversion and yield due to the variations of any operation variables. The study of variations in the optimal solution is known as post-optimality analysis or sensitivity analysis. In this case study, relative sensitivities are defined as following and applied to evaluate the optimal design problem.

$$\frac{\partial f_k}{\partial z_j}\frac{z_j^*}{f_k^*}, \quad k = 1, \ldots, 6 \tag{42}$$

where z_j is the jth operation variable as expressed in Eq. (26). Chen and Wang [40] have introduced a modified collocation method to evaluate both dynamic and static sensitivity analyses of biological systems. In this case, the method is applied to compute the relative steady-state sensitivities for overall productivity, glucose and xylose conversion, total sugar supply and residual glucose and xylose concentration with respect to a change in an operation variable. Fig. 2 shows the relative sensitivities for each operation variable. The insensitive variables are not shown in the figure. We

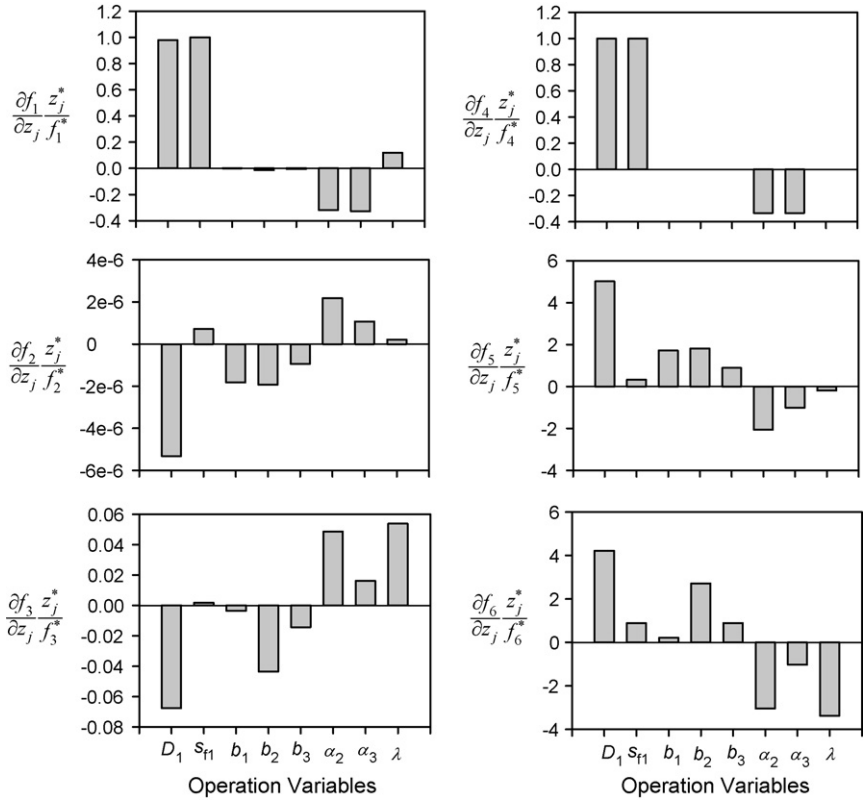

Fig. 2. Relative sensitivities of the overall productivity (f_1), glucose conversion (f_2), xylose conversion (f_3), total sugar supply (f_4), residual glucose (f_5) and residual xylose concentrations (f_6) with respect to the operation variables.

Table 2
Optimal results for the three-stage integrated extractive fermentation process with various lignocellulosic feedstocks. Each ratio λ for fed glucose concentration to fed sugar concentration is estimated from Jørgensen et al. [41].

Feedstocks	λ	f_1 (kg/m^3 h)	f_2	f_3	f_4 (kg/m^3 h)	f_5 (kg/m^3)	f_6 (kg/m^3)	D_1 (h^{-1})	s_{f1} (kg/m^3)	b_i
Agricultural waste										
Rice straw	0.58	11.335	1.0	0.971	26.012	7.009E−5	0.584	1.605	48.626	0.059
Switch grass	0.60	11.669	1.0	0.973	26.660	6.852E−5	0.627	1.354	59.065	0.071
Corn stover	0.65	11.749	1.0	0.984	26.503	4.473E−5	0.357	1.214	65.476	0.074
Sugarcane bagasse										
Wheat straw										
Hardwood										
Salix	0.74	11.851	1.0	0.993	26.297	2.560E−5	0.178	0.848	93.035	0.092
Cellulose wastes										
Paper sludge	0.79	11.908	1.0	0.995	26.184	1.661E−5	0.098	0.767	102.384	0.086
Softwood										
Pine	0.84	11.962	1.0	0.997	26.077	7.043E−6	0.038	0.813	96.250	0.062
Spruce	0.90	12.023	1.0	0.999	25.954	4.097E−6	0.008	0.956	81.427	0.051

observed that the dilution rate and fed sugar concentration are the most sensitive variables with respect to the objective functions and constraints. The overall productivity should be enhanced if both dilution rate and fed sugar concentration increase. Meanwhile, the residual glucose and xylose concentrations should be increased more. As a result, the overall satisfaction for all objective functions and constraints decreases. The relative sensitivities of the glucose conversion with respect to each operation variable are very small, which indicates that the glucose conversion is insensitive to the operation variables. The total sugar supply is independent of each bleed ratio because their relative sensitivities are zero. The volume ratios, α_2 and α_3, and the ratio, λ, for the fed glucose concentration to the fed sugar concentration seem to sensitive parameters observed from Fig. 2. We therefore consider the volume ratios as the decision variables in the optimization problem, and then to solve the problem again. The optimal solution is also shown in Case 4 of Table 1. The productivity and xylose conversion can be improved a little compared with Case 3. The optimal results shown in Table 1 are considered as λ = 0.65, which is estimated from corn stover as discussed in [41], we also consider various ratios to determine the optimal design as shown in Table 2. Higher glucose ratio of the feedstock can yield higher ethanol productivity and conversion.

We use Case 3 in Table 1 as example to explain the trade-off effect for the optimization problem. We first fixed the optimal solution obtained from Case 3, except dilution rate, to compute the overall productivity, conversion and constraints. Fig. 3 shows the computational results of the overall productivity, xylose conversion, sugar supply and residual xylose concentration with respect to various dilution rates. Glucose is almost completely exhausted by using various ratios of the dilution rate so that the glucose conversion (f_2) is nearly equal to one and residual glucose concentration (f_5) is smaller than 3.0E−4. As a result, both profiles are not shown in this figure. Similarly, Fig. 4 shows the computational results of the overall productivity, xylose conversion, sugar supply and residual xylose concentration with respect to various fed sugar concentrations, but the other operation variables are fixed at their optimal values. From the computational results, we observe that the productivity and residual xylose concentration increase, and xylose conversion decreases as the dilution rate increases. At first look from Fig. 3, we seem to be able to obtain the identical optimal solution if we consider a single objective function f_1 and a single constraint f_4, but the bounded value for the constraint needs to be specified in advance. In real applications, some optimal values are determined from optimization problems. We have to solve a series of the single optimization problem with using various bounded value for the constraint in order to achieve a trade-off solution. In contrast, the fuzzy goal attainment method is applied to find the trade-off solution between the intervals for the constraints. Table 3 shows a series of optimal solutions obtained from the crisp single optimization problem with using various bounded values s_t^B for the constraint f_4. If the bounded value is specified at 26.503, which was obtained from the optimal value by the fuzzy goal attainment method, we can achieve the identical solution to that of Case 3 in Table 1.

The mutation strategy in differential evolution and HDE uses the difference between two or four mutually independent individuals to create a search direction. As a result, the least population size for HDE is 3 or 5, which includes the parent individual. In this case, we also use the population size of 10 for HDE to solve the problem, i.e., Case 3 of Table 1. We obtained the nearly identical solution, but spent about 1.8-fold CPU time to that of Case 3 in Table 1. The HDE algorithm is a stochastic optimization method, and its optimal

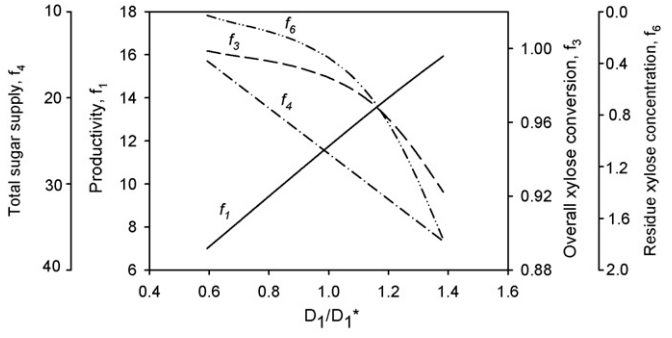

Fig. 3. The overall productivity (f_1), xylose conversion (f_3), total sugar supply (f_4), and residual xylose concentration (f_6) with respect to various ratios of dilution rate to the optimal dilution rate.

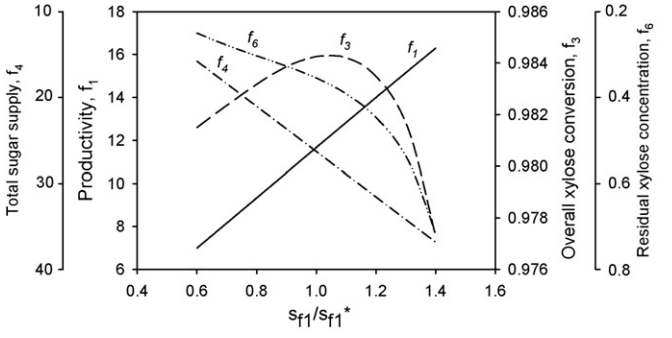

Fig. 4. The overall productivity (f_1), xylose conversion (f_3), total sugar supply (f_4) and residual xylose concentration (f_6) with respect to various ratios of the fed sugar concentration to the optimal value.

Table 3
Optimal results for maximizing the single objective function f_1 with using various bounded value s_t^B for the constraint f_4.

s_t^B	f_1 (kg/m^3 h)	f_2	f_3	f_4 (kg/m^3 h)	f_5 (kg/m^3)	f_6 (kg/m^3)	D_1 (h^{-1})
10	4.454	1.0	0.999	10.0	1.039E−6	8.020E−3	0.740
20	8.899	1.0	0.996	20.0	6.699E−6	0.048	1.694
26.503	11.749	1.0	0.984	26.503	4.149E−5	0.308	1.406
30	13.261	1.0	0.975	30.0	7.206E−5	0.442	1.743
40	14.783	1.0	0.957	33.635	1.340E−4	0.50	3.0

Table 4
Optimal results for the fuzzy optimization problem solved by HDE using different seeds to generate random numbers.

Run	f_1 (kg/m^3 h)	f_2	f_3	f_4 (kg/m^3 h)	f_5 (kg/m^3)	f_6 (kg/m^3)	D_1 (h^{-1})	s_{f1} (kg/m^3)	b_i
1	11.748	1.0	0.984	26.503	4.589E−5	0.381	1.150	69.133	0.079
2	11.749	1.0	0.984	26.503	4.427E−5	0.349	1.240	64.125	0.073
3	11.749	1.0	0.984	26.502	4.282E−5	0.326	1.325	59.997	0.067
4	11.749	1.0	0.984	26.502	4.163E−5	0.310	1.397	56.896	0.063
5	11.749	1.0	0.984	26.503	4.455E−5	0.354	1.224	64.951	0.074
Mean	11.7488	1.0	0.984	26.5026	4.3832E−5	0.3440	1.2672	63.0204	0.0712
Std	4.4721E−4	0.0	0.0	5.4772E−4	1.6444E−6	0.0273	0.0956	4.7159	0.0063

solution depends on random numbers. In this study, we used Compaq Visual Fortran (CVF) to implement the HDE algorithm so that the default in CVF was applied to generate random numbers for the stochastic searching. As a result, the optimal solutions for all computations are obtained from one run of HDE. We also applied the intrinsic procedure, RANDOM_SEED, in CVF to generate five different seeds, and then ran the same problem five times. Table 4 shows the optimal solution for each run. The mean of the five runs are nearly identical to that of Case 3 in Table 1. The standard deviations (std) for each item computed from the five runs are small.

The integrated process could be reduced into two simplified processes. In the first simplified fermentation process, referred to as continuous fermentation with cell recycling, each stage consists of a bioreactor and a cell-recycling unit. The material balance equations and the optimization formulation for the first simplified process could be straightforwardly obtained from the integrated process by assigning a value of zero to the extraction efficiency of each stage. The second simplified process is the continuous fermentation in series (i.e., the bleed ratio for each stage being one). Following similar procedures, we obtained the optimal solutions as shown in Table 5. For the continuous fermentations with cell recycling, we obtained the optimal productivity of 10.81 kg/m^3 h, glucose conversion of one, xylose conversion of 0.969 and total sugar supply of 24.503 kg/m^3 h. In addition, we retained the residual glucose concentration of 3.045E−5 kg/m^3 and xylose concentration of 0.337 kg/m^3. The overall productivity for the first simplified process (Process I of Table 5) is 8.0% less than that obtained for the integrated extractive fermentation with cell recycling, as shown in Case 3 of Table 1, because ethanol is extracted from the extractor *in situ* to alleviate product inhibition.

Process II-a in Table 5 shows the optimal solution for the three-stage continuous fermentation without cell recycling. The overall productivity for the integrated process was about 13-fold higher than that of the second simplified continuous fermentation process due to a lower dilution rate. Moreover, the residual xylose concentration of 2.532 kg/m^3 did not satisfy the desired upper bound such that the design was completely unacceptable. Krishnan [30] carried out batch fermentation experiments using the yeast 1400 (pLNH33) to convert glucose and xylose to ethanol and obtained an ethanol productivity of 0.91 kg/m^3 h, which was about equal to that of the continuous fermentation process without cell recycling. In terms of concentration characteristics, a continuously stirred tank bioreactor in series is similar to a tubular reactor [42]. We therefore considered a seven-stage continuous fermentation process without cell recycling to evaluate the ethanol productivity. The optimal productivity of 1.055 kg/m^3 h, xylose conversion of 0.899 and residual xylose concentration of 2.279 kg/m^3 were obtained, as listed in Case II-b of Table 5. These results did not satisfy the desired lower/upper bounds such that the design was completely unacceptable.

Table 5
The optimal results for continuous fermentation processes with/without cell recycling. Process I is the continuous fermentation with cell recycling. Process II-a is the three-stage continuous fermentation without cell recycling, and Process II-b is the seven-stage continuous fermentation without cell recycling. The values in parentheses indicate the optimal grades of the membership function for each objective and constraint.

Process	I	II-a	II-b
Productivity (kg/m^3 h)	10.810 (0.508)	0.886 (0.0)	1.055 (0.0)
Glucose conversion	1.0 (1.0)	1.0 (1.0)	1.0 (1.0)
Xylose conversion	0.969 (0.508)	0.872 (0.0)	0.899 (0.0)
Sugar supply (kg/m^3 h)	24.503 (0.638)	2.073 (1.0)	2.446 (1.0)
Residual glucose conc. (kg/m^3)	3.045E−5 (1.0)	1.253E−4 (1.0)	1.124E−9 (1.0)
Residual xylose conc. (kg/m^3)	0.337 (1.0)	2.532 (0.0)	2.279 (0.0)
Dilution rate (h^{-1})	2.317	0.110	0.266
Fed sugar conc. (kg/m^3)	31.717	56.458	64.364
Bleed ratio	0.032	1.0	1.0

5. Conclusion

Ethanol from lignocellulosic materials holds great promise as a renewable fuel and has the potential to make a significant contribution to the solution of major renewable energy and environmental problems. Lignocellulosic materials contain glucose and xylose as the major fermentable sugars. Several cell culture strategies have been applied to ethanol fermentation processes in order to improve productivity. In this study, we introduced an integrated extractive fermentation with cell recycling for ethanol production using the genetically engineered *Sacchromyces* yeast 1400 (pLNH33), which can utilize glucose and xylose as carbon sources to produce ethanol; this strategy allows for maximum satisfaction for all design requirements, such as overall productivity, overall glucose and xylose conversions, total sugar supply and residual glucose and xylose concentrations. The trade-off multiobjective optimization is formulated as a fuzzy goal attainment problem. In the case studies, we considered the three-stage integrated process using various operation variables to determine optimal design. The optimal design was achieved to the overall satisfaction of 57.3% if the dilution rate, fed glucose concentration and bleed ratio were considered as the design variables. The optimal productivity was 2.8-fold higher

than that of the tradeoff optimal design problem using the dilution rate as the only operation variable. The integrated process could be reduced into two simplified processes. The integrated extractive fermentation with cell recycling involved extracting ethanol from the extractor *in situ* to alleviate product inhibition such that the optimal overall productivity was 8.0% higher than that obtained by the continuous fermentation with cell recycling, and about 13-fold higher than that of the continuous fermentation without cell recycling.

The relative sensitivities for each objective function and its constraints with respect to a change in each design variable were evaluated based on their effects on variations in the optimal design. We observed that the dilution rate and fed sugar concentration are the most sensitive variables with respect to the objective functions and constraints. The overall productivity should be enhanced if both dilution rate and fed sugar concentration increase. Meanwhile, the residual glucose and xylose concentrations should be increased more. As a result, the overall satisfactory grade for all objective functions and constraints decreases.

Acknowledgment

Financial support from the National Science Council, ROC (Grant NSC 97-2221-E-194-010-MY3) is highly appreciated.

References

[1] M.S. Krishnan, Y. Xia, N.W.Y. Ho, G.T. Tsao, Fuel ethanol production from lignocellulosic sugars: studies using a genetically engineered *Saccharomyces* yeast, ACS Symp. Ser. 666 (1997) 74–92.
[2] J. Lee, Biological conversion of lignocellulosic biomass to ethanol, J. Biotechnol. 56 (1997) 1–24.
[3] L. Olsson, B. Hahn-Hagerdal, Fermentation of lignocellulosic hydrolysates for ethanol production, Enzyme Microb. Technol. 18 (1996) 312–331.
[4] C.A. Cardona, O.J. Sanchez, Fuel ethanol production: process design trends and integration opportunities, Bioresour. Technol. 98 (2007) 2415–2457.
[5] J. Zaldivar, J. Nielsen, L. Olsson, Fuel ethanol production from lignocellulose: a challenge for metabolic engineering and process integration, Appl. Microbiol. Biotechnol. 56 (2001) 17–34.
[6] R. Bura, Bioconversion of corn fibre to ethanol, Ph.D. Dissertation, British Columbia University, 2004.
[7] C.N. Hamelinck, G. Van Hooijdonk, A.P.C. Faaij, Ethanol from lignocellulosic biomass: techno-economic performance in short-, middle- and long-term, Biomass Bioenergy 28 (2005) 384–410.
[8] R Purwadi, T. Brandberg, M.J. Taherzadeh, A possible industrial solution to ferment lignocellulosic hydrolyzate to ethanol: continuous cultivation with flocculating yeast, Int. J. Mol. Sci. 8 (2007) 920–932.
[9] J.C. du Preez, M. Bosch, B.A. Prior, The fermentation of hexose and pentose sugars by *Candida shehatae* and *Pichia stipitis*, Appl. Microbiol. Biotech. 23 (1986) 228–233.
[10] A. Asghari, R.J. Bothast, J.B. Doran, L.O. Ingram, Ethanol production from hemicellulose hydrolysates of agricultural residues using genetically engineered *Escherichia coli* strain KO11, J. Ind. Microbiol. Biotechnol. 16 (1996) 42–47.
[11] M. Bertilsson, J. Andersson, G. Lidén, Modeling simultaneous glucose and xylose uptake in *Saccharomyces cerevisiae* from kinetics and gene expression of sugar transporters, Bioprocess Biosyst. Eng. 31 (2008) 369–377.
[12] N. Leksawasdi, E.L. Joachimsthal, P.L. Rogers, Mathematical modelling of ethanol production from glucose/xylose mixtures by recombinant *Zymomonas mobilis*, Biotechnol. Lett. 23 (2001) 1087–1093.
[13] R. Purwadia, M.J. Taherzadeha, The performance of serial bioreactors in rapid continuous production of ethanol from dilute-acid hydrolyzates using immobilized cells, Bioresour. Technol. 99 (2008) 2226–2233.
[14] Y. Zhao, Y.H. Lin, The growth of *Saccharomyces cerevisiae* in a chemostat under high glucose conditions, Biotechnol. Lett. 25 (2003) 1151–1154.
[15] C. Lafforgue-Delorme, P. Delorme, G. Goma, Continuous alcoholic fermentation with recycle by tangential filtration: key points for process modeling, Biotechnol. Lett. 16 (1994) 741–746.
[16] S.C. Oliveira, H.F. De Castro, A.E.S. Visconti, R. Giudici, Continuous ethanol fermentation in a tower reactor with flocculating yeast recycle: scale-up effects on process performance, kinetic parameters and model predictions, Bioprocess Eng. 20 (1999) 157–160.
[17] T.C.B Paiva, S. Sato, A.E.S. Visconti, L.A.B. Castro, Continuous alcoholic fermentation process in a tower reactor with recycling of flocculating yeast, Appl. Biochem. Biotechnol. 57/58 (1996) 535–541.
[18] A. Nishiwaki, I.J. Dunn, Performance of a multistage fermentor with cell recycle for continuous ethanol production, Chem. Eng. Commun. 162 (1997) 179–198.
[19] A. Nishiwaki, I.J. Dunn, Operating conditions for high production rates of ethanol in a continuous two-stage fermenter with cell recycle, Can. J. Chem. Eng. 83 (2005) 903–908.
[20] C. Roca, L. Olsson, Increasing ethanol productivity during xylose fermentation by cell recycling of recombinant *Saccharomyces cerevisiae*, Appl. Microbiol. Biotechnol. 60 (2003) 560–563.
[21] P. Garhyan, S.S.E.H. Elnashaie, Bifurcation analysis of two continuous membrane fermentor configurations for producing ethanol, Chem. Eng. Sci. 59 (2004) 3235–3268.
[22] F.L.H. Silva, M.I. Rodrigues, F. Maugeri, Dynamic modelling, simulation and optimization of an extractive continuous alcoholic fermentation, J. Chem. Tech. Biotechnol. 74 (1999) 176–182.
[23] R.D. Offeman, S.K. Stephenson, G.H. Robertson, J.O. William, Solvent extraction of ethanol from aqueous solutions. I. Screening methodology for solvents, Ind. Eng. Chem. Res. 44 (2005) 6789–6796.
[24] M. Kilic, E. Bayraktar, S. Ates, U. Mehmetoglu, Investigation of extractive citric acid fermentation using response-surface methodology, Process Biochem. 27 (2002) 759–767.
[25] A.J. Daugulis, D.B. Axford, P.J. McLellan, Economics of ethanol production by extractive fermentation, Can. J. Chem. Eng. 69 (1991) 488–497.
[26] M. Gyamerah, J. Glover, Production of ethanol by continuous fermentation and liquid–liquid extraction, J. Chem. Technol. Biotechnol. 66 (1996) 145–152.
[27] V.M. Yabannavar, D.I.C. Wang, Strategies for reducing solvent toxicity in extractive fermentations, Biotechnol. Bioeng. 37 (1991) 716–722.
[28] H.C. Cheng, F.S. Wang, Trade-off optimal design of a biocompatible solvent for an extractive fermentation process, Chem. Eng. Sci. 62 (2007) 4316–4324.
[29] H.T. Lin, F.S. Wang, Optimal design of an integrated fermentation process for lactic acid production, AIChE J. 53 (2007) 449–459.
[30] M.S. Krishnan, Process development of fuel ethanol production from lignocellulosic sugars using genetically engineered yeasts, Ph.D. Dissertation, Purdue University, 1996.
[31] H.C. Cheng, F.S. Wang, Optimal biocompatible solvent design for a two-stage extractive fermentation process with cell recycling, Comput. Chem. Eng. 32/7 (2008) 1385–1396.
[32] N.M.Y. Ho, G. T. Tsao, Recombinant yeasts for effective fermentation of glucose and xylose, U.S. PCT Patent No. W095/13362, 1995.
[33] M.S. Krishnan, Y. Xia, N.W.Y. Ho, G.T. Tsao, Fermentation kinetics of ethanol production from glucose and xylose by recombinant *Saccharomyces* 1400 (pLNH33), Appl. Biochem. Biotechnol. 77/79 (1999) 373–388.
[34] M.K. Krokida, C.T. Kiranoudis, Pareto design of fluidized bed dryers, Chem. Eng. J. 79 (2000) 1–12.
[35] Y. Sawaragi, H. Nakayama, T. Tanino, Theory of Multiobjective Optimization, Academic Press, London, 1985.
[36] M. Sakawa, Fuzzy Sets and Interactive Multiobjective Optimization, Plenum Press, New York, 1993.
[37] F.S. Wang, K.J. Lin, Performance analysis and fuzzy optimization of a two-stage fermentation process with cell recycling including an extractor for lactic acid production, Chem. Eng. Sci. 58 (2003) 3753–3763.
[38] F.S. Wang, C.H. Jing, Fuzzy-decision-making problems of fuel ethanol production using a genetically engineered yeast, Ind. Eng. Chem. Res. 37 (1998) 3434–3443.
[39] J.P. Chiou, F.S. Wang, Hybrid method of evolution algorithms for static and dynamic optimization problems with application to a fed batch fermentation process, Comput. Chem. Eng. 23 (1999) 1277–1291.
[40] M.L. Chen, F.S. Wang, Dynamic sensitivity analysis of biochemical oscillation networks using modified collocation method, J. Taiwan Inst. Chem. Eng. 40 (2009) 371–379.
[41] H. Jørgensen, J.B. Kristensen, C. Felby, Enzymatic conversion of lignocellulose into fermentable sugars: challenges and opportunities, Biofuels, Bioprod. Biorefin. 1 (2007) 119–134.
[42] I.J. Dunn, E. Heinzle, J. Ingham, J.E. Přenosil, Biological Reaction Engineering, Wiley-VCH, 2003.